

Milliarcsecond Core Size Dependence of the Radio Variability of Blazars

Po-Chih Hsu (許博智)^{1,2}, Jun Yi (Kevin) Koay¹, Chorng-Yuan Hwang², and Satoki Matsushita¹

¹Institute of Astronomy and Astrophysics, Academia Sinica

²Graduate Institute of Astronomy, National Central University

Introduction

Studying AGN variability on timescales of months to years enables us to better understand the sub-parsec-scale structure of AGNs, and the physics of supermassive black holes. In this study, we focus on the radio variability of 1158 blazars, which were observed at 15 GHz through the Owens Valley Radio Observatory (OVRO) Blazar Monitoring Program (Richards et al., 2011), where these sources have been observed about twice a week over a decade. In this study, we deconvolute 1 GHz scattering core sizes from the observed core sizes, getting the intrinsic core sizes of the source, and investigate the dependence of variability amplitudes and timescales on 1 GHz intrinsic/scattering/observed core sizes, by using the milliarcsecond core sizes (538 sources overlap) measured using Very Long Baseline Interferometry (VLBI) from Koryukova et al. (2022), which is the extension work of Pushkarev & Kovalev (2015).

Analysis

- We used structure function (SF) to characterize variation of source light curve
- Using SF model fit to derive characteristic timescale (τ_{char}), as well as variability amplitude at 1000 days ($D(1000\text{d})$)

$$D_{\text{mod}}(\tau) = D(1000\text{d}) \frac{1 + \tau_{\text{char}}/1000}{1 + \tau_{\text{char}}/\tau} + D_{\text{noise}}$$

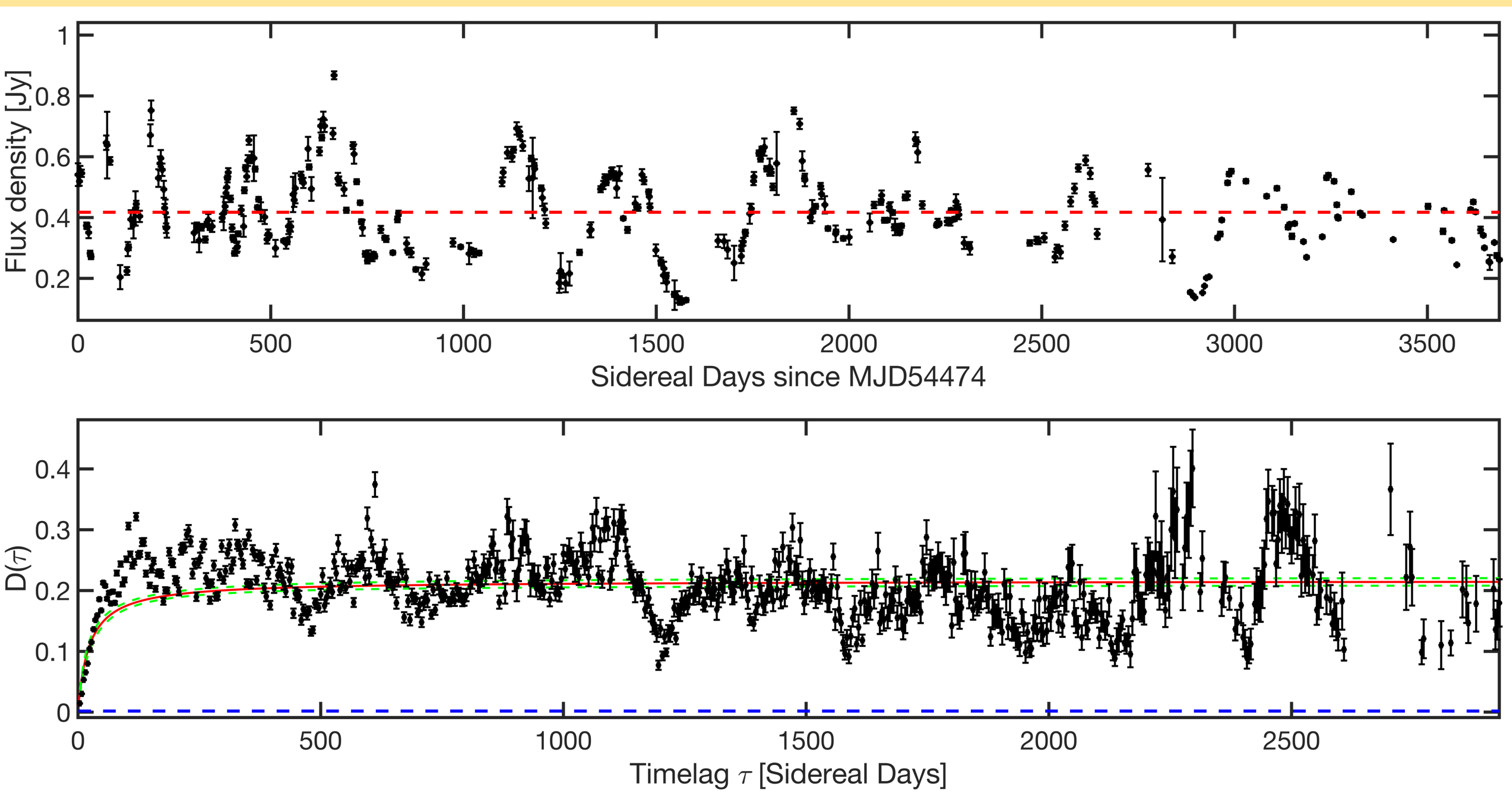


Figure 1.

Light curve (top) and SF (bottom) of a blazar source J1135-0428. Red dashed line in the upper panel displays the mean flux density. Red solid line in the lower panel shows the SF model fit; green dashed line shows 95% confident bounds for the fit, and blue dashed line shows the SF systematic and instrumental errors (D_{noise}).

- Core sizes were obtained from VLBI derived by Koryukova et al., 2022 (extension of work by Pushkarev & Kovalev, 2015) at 1 GHz.
- Using core size-frequency relationship and core sizes convolution relationship, can derive deconvoluted scattering core size (intrinsic core size).

Core size-frequency relationship $\theta \propto \nu^{-k}$, $\begin{cases} \text{scattering, } k = 2 \\ \text{intrinsic, } k = 1 \end{cases}$

Core sizes Convolution relationship $\theta_{\text{obs}}^2 = \theta_{\text{int}}^2 + \theta_{\text{sca}}^2$

Results

After we deconvoluted scattering core sizes (figure 2 middle panel) from the observed core sizes (figure 2 right panel), 1 GHz intrinsic core sizes (figure 2 left panel) are significantly correlated with 15 GHz $D(1000\text{d})$.

Conclusion

In previous study, significant correlation was found between 15 GHz $D(1000\text{d})$ and core sizes greater than 8 GHz. However, weak dependence at low frequencies (i.e., 2 and 5 GHz) were found, due to scatter broadening from ISM. After deconvoluting $\theta_{\text{sca},1\text{ GHz}}$ from $\theta_{\text{obs},1\text{ GHz}}$, and get $\theta_{\text{inc},1\text{ GHz}}$. We found that $\theta_{\text{int},1\text{ GHz}}$ are significantly correlated with 15 GHz $D(1000\text{d})$. Also, distribution of strong and weak variables of $\theta_{\text{int},1\text{ GHz}}$ show up significant different, so does the distribution of fast and slow variables of $\theta_{\text{int},1\text{ GHz}}$.

In previous study (Hsu et al., in prep):

- Low-frequency observed core sizes has less significant correlation with $D(1000\text{d})$ compare to high-frequency ones
 - $D(1000\text{d})$ v.s. $\theta_{\text{obs},2\text{ GHz}}$: $r = -0.15$; $p = 1.82 \times 10^{-5}$
 - $D(1000\text{d})$ v.s. $\theta_{\text{obs},15\text{ GHz}}$: $r = -0.52$; $p = 1.74 \times 10^{-27}$
- Distribution of strong and weak variables (separated by $\tilde{D}(1000\text{d})$) of low-frequency observed core sizes are less significant
 - $\theta_{\text{obs},2\text{ GHz strong}}$ v.s. $\theta_{\text{obs},2\text{ GHz weak}}$: $p = 1.83 \times 10^{-2}$
 - $\theta_{\text{obs},15\text{ GHz strong}}$ v.s. $\theta_{\text{obs},15\text{ GHz weak}}$: $p = 2.58 \times 10^{-15}$
- Distribution of fast and slow variables (separated by $\tilde{\tau}_{\text{char}}$) of low-frequency observed core sizes have less significance
 - $\theta_{\text{obs},2\text{ GHz fast}}$ v.s. $\theta_{\text{obs},2\text{ GHz slow}}$: $p = 4.72 \times 10^{-4}$
 - $\theta_{\text{obs},15\text{ GHz fast}}$ v.s. $\theta_{\text{obs},15\text{ GHz slow}}$: $p = 2.33 \times 10^{-6}$

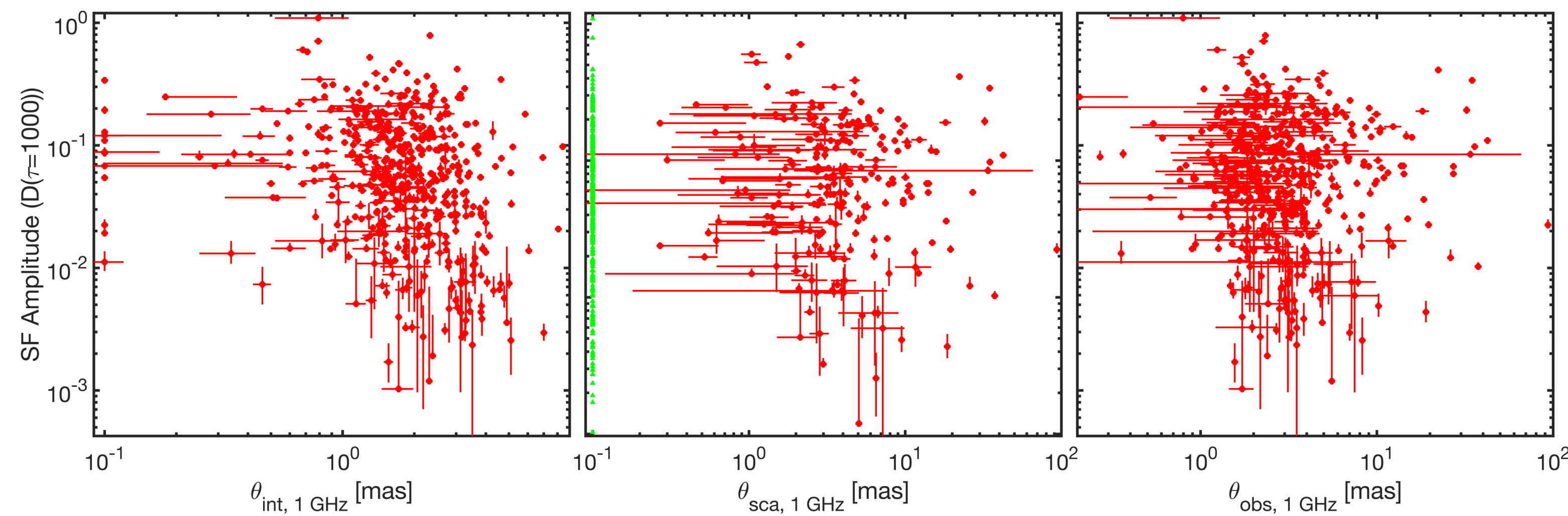


Figure 2.

Scattering plot of long term variability amplitudes ($D(1000\text{d})$) on 1 GHz intrinsic (left panel), scattering (middle panel), and observed (right panel) core sizes, which are derived from Koryukova et al., 2022. Green triangles in the middle panel are sources with insignificant scattering, are placed with upper limit ($\theta_{\text{sca},1\text{ GHz}} = 0.1\text{ mas}$).

1 GHz intrinsic/scattering/observed core sizes were separated into strong and weak variables (separated by $\tilde{D}(1000\text{d})$), as well as fast and slow variables (separated by $\tilde{\tau}_{\text{char}}$). Two sample K-S test results are shown in table 1.

- $\theta_{\text{int},1\text{ GHz strong}}$ has significantly smaller core size than $\theta_{\text{int},1\text{ GHz weak}}$
- $\theta_{\text{int},1\text{ GHz fast}}$ has significantly smaller core sizes than $\theta_{\text{int},1\text{ GHz slow}}$

Table 1.

Result of correlation test and two sample K-S test. Test A presents the correlation test results of the scattering plot in figure 2; test B exhibits the two sample K-S test results of the strong and weak variable core sizes (separated by $\tilde{D}(1000\text{d})$); test C displays the two sample K-S test result of core sizes of fast and slow variables (separated by $\tilde{\tau}_{\text{char}}$). $\theta_{\text{sca},1\text{ GHz}} = 0.1\text{ mas}$ are upper limits, which were excluded from all of the tests.

test A	sample number	correlation coefficient	p-value
$D(1000\text{d})$ v.s. $\theta_{\text{int},1\text{ GHz}}$	538	-0.2915	5.34×10^{-12}
$D(1000\text{d})$ v.s. $\theta_{\text{sca},1\text{ GHz}}$	230	0.0661	3.18×10^{-1}
$D(1000\text{d})$ v.s. $\theta_{\text{obs},1\text{ GHz}}$	538	-0.0669	1.21×10^{-1}
test B (distributed by $\tilde{D}(1000\text{d})$)	sample number	$\tilde{D}(1000\text{d})$	p-value
Distribution of $\theta_{\text{int},1\text{ GHz strong}}$ and $\theta_{\text{int},1\text{ GHz weak}}$	538	0.0601	3.58×10^{-6}
Distribution of $\theta_{\text{sca},1\text{ GHz strong}}$ and $\theta_{\text{sca},1\text{ GHz weak}}$	230	0.0601	9.35×10^{-1}
Distribution of $\theta_{\text{obs},1\text{ GHz strong}}$ and $\theta_{\text{obs},1\text{ GHz weak}}$	538	0.0601	3.16×10^{-1}
test C (distributed by $\tilde{\tau}_{\text{char}}$)	sample number	$\tilde{\tau}_{\text{char}}$	p-value
Distribution of $\theta_{\text{int},1\text{ GHz fast}}$ and $\theta_{\text{int},1\text{ GHz slow}}$	538	633 d	2.45×10^{-2}
Distribution of $\theta_{\text{sca},1\text{ GHz fast}}$ and $\theta_{\text{sca},1\text{ GHz slow}}$	230	550 d	1.48×10^{-1}
Distribution of $\theta_{\text{obs},1\text{ GHz fast}}$ and $\theta_{\text{obs},1\text{ GHz slow}}$	538	633 d	4.99×10^{-1}

References

- Richards J. L. et al., 2011, ApJS, 194, 29
- Richards J. L. et al., 2014, MNRAS, 438, 3058
- Koryukova T. A. et al., 2022, MNRAS, 515, 1736
- Pushkarev A. B., Kovalev Y. Y., 2015, MNRAS, 452, 4274

Acknowledgment

This research has made use of data from the OVRO 40-m monitoring program (Richards, J. L. et al., 2011, ApJS, 194, 29), supported by private funding from the California Institute of Technology and the Max Planck Institute for Radio Astronomy, and by NASA grants NNX08AW31G, NNX11A043G, and NNX14AQ89G and NSF grants AST-0808050 and AST- 1109911.